The nature and origin of interstellar diamond

David F. Blake*, Friedemann Freund*,
Kannan F. M. Krishnan†, Charles J. Echer†,
Ruth Shipp*, Theodore E. Bunch*,
Alexander G. Tielens*, Robert J. Lipari‡,
Crispin J. D. Hetherington† & Sherwood Chang*

* NASA Ames Research Center, Moffett Field, California 94035, USA
† National Center for Electron Microscopy,
Lawrence Berkeley Laboratory, Berkeley, California 94720, USA
‡ Surface Science Laboratories, Mountain View, California 94043, USA

Microscopic diamond was recently discovered[1] in oxidized acid residues from several carbonaceous chondrite meteorites (for example, the Cδ component[2] of the Allende meteorite). Some of the reported properties of Cδ seem in conflict with those expected of diamond[1,3]. Here we present high spatial resolution analytical data which may help to explain such results. The Cδ diamond is an extremely fine-grained (0.5–10 nm) single-phase material, but surface and interfacial carbon atoms, which may comprise as much as 25% of the total, impart an 'amorphous' character to some spectral data. These data support the proposed high-pressure conversion of amorphous carbon and graphite into diamonds due to grain–grain collisions in the interstellar medium[4] although a low-pressure mechanism of formation cannot be ruled out.

The presence of krypton and nitrogen as well as isotopically anomalous xenon ('CCFXe', or 'Xe-HL') in the Cδ residue[5,6] has been interpreted to mean that the diamond is interstellar in origin[1,2]. Several low-pressure[1,7,8] as well as high-pressure[4] mechanisms of formation for interstellar diamond have been discussed.

Fragments of the Allende CV3 meteorite were treated with acid and oxidant using a method similar to that in Lewis *et al.*[1]. Preliminary observations revealed the presence of an apparent amorphous phase containing silicon and oxygen in addition to the diamond. The Si–O material was removed by further acid treatment. Diamond was identified by selected area electron diffraction. Diamond masses, 10–500 nm size, were observed. Scanning electron microscopy of these masses revealed tightly packed microcrystallites and an apparent lack of porosity. Bright and dark-field transmission electron microscopy (TEM) of these masses revealed 0.5–10.0 nm crystallites with irregular morphology. Microdiffraction using a 20-nm stationary probe (Fig. 1) yielded a Debye–Scherrer powder pattern of diamond with superimposed single crystal spots, confirming the exceptionally small grain size of most crystals and the presence of a few larger individuals. The *a* parameter (the length of the cube edge) is 0.365 nm, about 2% larger than the published value of 0.35667 nm. This increase in the lattice constant is consistent with very small diamond crystallites, as Vanderbilt and Louie[9] predict an increase in the C–C bond length by as much as 8.1% within the first two atomic layers of a free diamond surface. High-resolution TEM images of {111} planes of the Cδ diamond (Fig. 2) do show 2–4 nm tightly joined crystallites separated from one another by apparently structureless regions which may represent either crystallites in non-diffracting orientations, disordered interfacial regions, or both.

Analytical electron microscope microanalyses, using an energy-dispersive X-ray detector sensitive to all elements above boron in atomic number, showed that O and possibly N are the only impurities consistently present above 0.1–0.2%. The presence of substitutional N at 0.25% or less is supported by electron spectroscopy for chemical analysis (ESCA) and optical fluorescence studies on bulk Cδ material. According to Carey *et al.*[10] the H concentration measured by ion-probe analysis may exceed that of O by an order of magnitude.

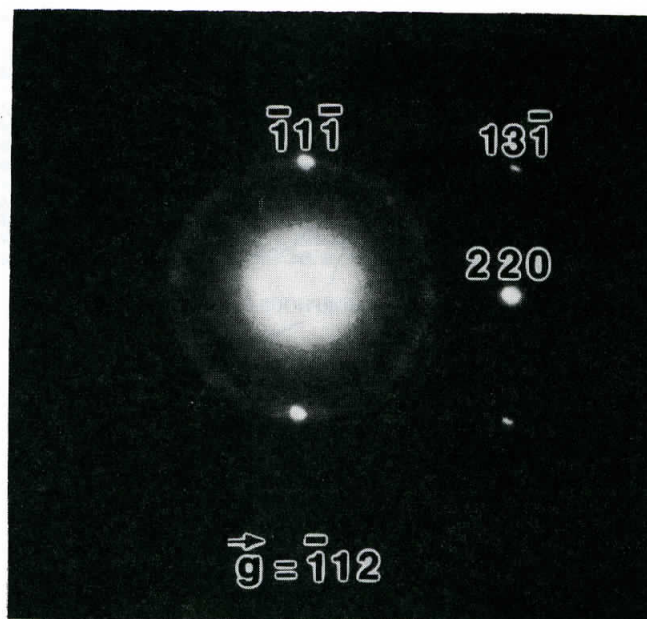Figure 3 shows electron-energy-loss spectra (EELS) from

Fig. 1 Microdiffraction pattern from Allende Cδ diamond. (001), (011), and (112) orientations were obtained; only the (112) direction is shown.
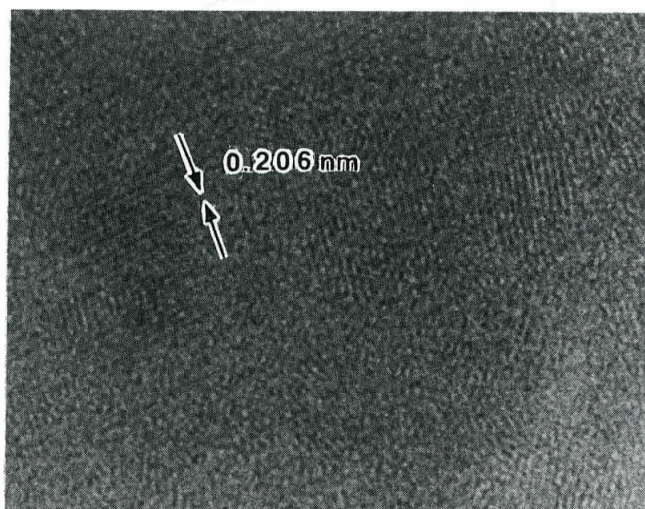

Fig. 2 High-resolution lattice image of (111) planes in a polycrystalline mass of Cδ diamond. The microcrystallites are surrounded by apparently structureless regions and diamond crystallites in non-diffracting orientations.

different forms of carbon. A comparison of the C K edge shape and fine structure showed Cδ diamond masses to be largely diamond, but with a significant pre-edge absorption feature indicative of transitions of C 1s electrons into π^* orbitals. Such π^* states are absent in ideal sp^3-bonded diamond but present in amorphous carbon, in graphite and at diamond surfaces as a result of restructuring[9,11].

Figure 4 shows that the ESCA spectrum of Cδ exhibits a $\pi \Rightarrow \pi^*$ shake-up satellite arising from C 1s photoelectrons which suffer an energy loss by exciting a π electron into a π^* orbital. Since purely sp^3-bonded diamond lacks π states, the presence of such a shake-up peak may be an indication of restructured π-type C–C bonds at grain-grain interfaces (such as at the surface of diamond crystallites[9,11]), or of sp^2 bonds in graphitic or 'amorphous' regions. The increased width of the C 1s peak is due to C atoms in slightly different environments. If one assumes a crystallite size of 2 nm, and if the restructuring affects three atom-layers, as many as 25% of all C atoms in Cδ
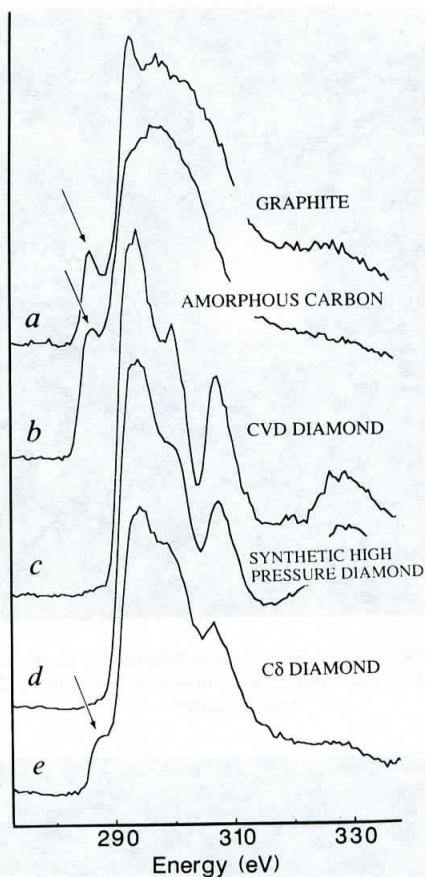
Fig. 3 EEL spectra for a number of carbon phases, showing the region in the vicinity of the carbon K edge. The region between 285 and 315 eV contains interpretable fine structure. Above 315 eV, multiple scattering (that is, thickness effects) dominates. a, Highly ordered pyrolitic graphite. b, Amorphous arc-sputtered carbon. c, Synthetic low-pressure CVD diamond (sample kindly provided by Dr R. Messier, Pennsylvania State University). d, Synthetic high pressure diamond. e, Cδ diamond. Some chemical shifts in the carbon K edge are apparent between spectra. A significant pre-ionization edge structure is present in the graphite, amorphous carbon, and Cδ diamond spectra (arrowed), representing carbon $1s \Rightarrow \pi^*$ transitions which are not allowed in the true diamond structure.

Fig. 4 ESCA spectra of the carbon 1s peak region of graphite, amorphous carbon and diamond materials (spectra aligned with reference to published carbon 1s-binding energies for graphite and diamond). Dotted lines indicate computer-generated gaussian peaks fitted to observed data. a, Highly ordered pyrolitic graphite. Note diffuse nature of $\pi \Rightarrow \pi^*$ shake-up satellites and asymmetry of measured peak. Peak width approaches instrumental resolution of 0.7 eV. b, Amorphous arc-sputtered carbon. Note marked asymmetry on high-energy side of peak. c, Synthetic low-pressure CVD diamond film. d, Gem-quality natural diamond. Note absence of $\pi \Rightarrow \pi^*$ shake-up satellite. Width slightly increased due to charging. e, Cδ, showing a narrow shake-up satellite at 289 eV. The carbon 1s peak can be separated into two main components, probably due to carbon atoms in the bulk and in the interfacial regions.

diamond would have electron states different from C atoms in the bulk. We therefore suggest on the basis of high resolution TEM, EELS and ESCA data, that the Cδ diamond is single phase, but with a significant contribution from C atoms at and near tightly interlocked grain-grain interfaces which lend an apparent amorphous character to EELS and ESCA spectra.

Lewis et al.[1] suggest that the Cδ diamond was formed at low pressure, by processes similar to those used in recent low-pressure chemical vapour deposition (CVD) laboratory syntheses[12]. The CVD diamond we have characterized by electron microscopic techniques is comprised of large (>1 μm) euhedral crystals which are quite unlike Cδ diamond. However, low-pressure diamond formation can occur under a wide variety of conditions resulting in a range of microstructural features. We therefore cannot exclude a low pressure mechanism of formation. Rather, we cite a second possible mechanism of diamond formation in interstellar space. High velocity (>10 km s^{-1}) grain-grain collisions behind supernova shock waves[4] provide the high pressures required to convert amorphous or graphitic carbon grains into diamonds[13]. According to the grain-grain collision model, this conversion takes place by melting of carbon in the diamond stability field and extremely rapid crystallization from many nucleation sites. During crystallization, impurities that may be present in the original grain, for example krypton
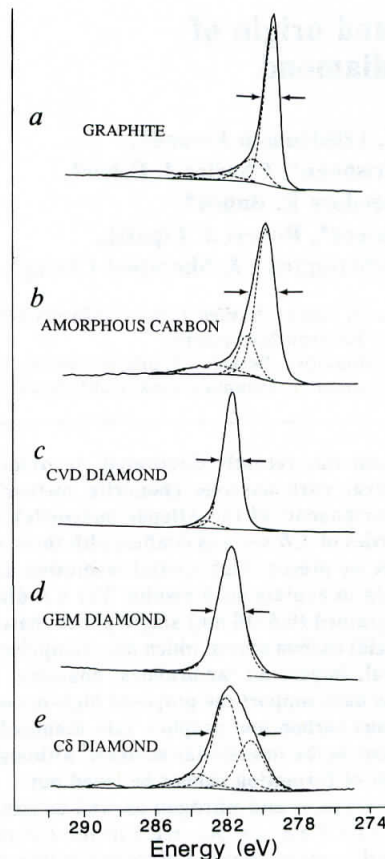
and xenon, adsorbed to amorphous or graphitic carbon, are expected to be excluded and to become trapped in the interfacial regions between diamond crystallites, while nitrogen may enter substitutional sites in the diamond structure. The prediction of the model regarding the grain size of the resulting diamonds is consistent with the TEM data showing the Cδ diamond to consist of 0.5–10 nm, tightly joined, well crystallized microcrystallites. The cryptocrystalline nature of the Cδ diamond masses, plus the apparent lack of porosity, strongly argue against agglomeration of pre-formed diamond crystallites through sintering.

The bulk of the carbon in primitive meteorites occurs as acid-insoluble, fine-grained particulate matter. The mechanisms for production of this material under solar nebula conditions are poorly understood[14]. It has previously been suggested that pre-solar origins can account for the minor fraction of the carbonaceous components that contain unusual isotopic ratios for H, C or N[15]. An interstellar origin for the Cδ diamond, whic contains isotopically 'ordinary' carbon[10], however, emphasizes the possibility that most of the reduced carbonaceous particles in primitive meteorites had a similar origin.

It remains to find diamond in situ in carbonaceous chondrite meteorites so that detailed petrographic investigations of textural relationships between diamond and other phases can be carried out. In addition, a further characterization of low press-

ure diamond is necessary to determine the range of structures and chemistries resulting from these non-equilibrium processes.

1. Lewis, R. S., Tang, M., Wacker, J. F., Anders, E. & Steel, E. *Nature* **326,** 160–162 (1987).
2. Swart, P. K., Gradyk, M. M., Pillinger, C. T., Lewis, R. S. & Anders, E. *Science* **220,** 406–410 (1983).
3. Ash, R. D. *Meteoritics* **22,** (in the press).
4. Tielens, A. G. G. M., Seab, C. G., Hollenbach, D. J. & McKee, C. *Astrophys. J. Lett.* **319,** L103 (1987).
5. Ott, U., Mack, R. & Chang, S. *Geochim. cosmochim. Acta* **45,** 1751–1788 (1981).
6. Lewis, R. S., Anders, E., Wright, I. P., Norris, S. J. & Pillinger, C. T. *Nature* **305,** 767–771 (1983).
7. Hecht, J. H. *Nature* **328,** 765 (1987).
8. Nuth, J. A. *Nature* **329,** 589 (1987).
9. Vanderbilt, D. & Louie, S. G. *Phys. Rev.* **B30,** 6118–6130 (1984).
10. Carey, W., Zinner, E. & Lewis, R. *Meteoritics* **22,** (in the press).
11. Morar, J. F. *et al. Phys. Rev.* **B33,** 1346–1350 (1986).
12. Roy, R. *Nature* **325,** 17–18 (1987).
13. DeCarli, P. S. & Jamieson, J. C. *Science* **133,** 1821 (1961).
14. Kerridge, J. F., Shipp, R. & Chang, S. *Geochim. cosmochim. Acta* **51,** 2527–2540 (1987).
15. Lewis, R. S. & Anders, E. *Scient. Am.* **249,** 66–77 (1983).